

Synthesis, Characterization, and Oxidation Catalysis Studies of a Monofunctionalized Copper Pyridine-Aza Macrocycle

McKenzie, Severin G^{†*}, Palluccio, Taryn, D[†]., Patterson, John D[†]., Rybak-Akimova, Elena V[†].

[†]Tufts University, 62 Talbot Avenue, Medford, MA 02155

* Corresponding author. (e-mail: severin.mckenzie@tufts.edu; mailing address: 15 Carmel Street (2), Mission Hill, MA 02120)

Abstract

A copper-containing pyridine-aza macrocycle (PyMACs) with a propionic acid functionality was synthesized and characterized using X-ray crystallography and various spectroscopic techniques. The complex was then screened for peroxidase, olefin epoxidation, and phenol oxidation properties, using an ABTS assay, GC-MS, and UV-Vis spectrophotometry, respectively. The control copper (II) perchlorate salts were superior oxidation catalysts to the pentadentate carboxylic acid complex, CuLCOOH, and the unfunctionalized amine PyMAC, CuCRH. This might indicate that free copper ions facilitate the one-electron oxidations necessary for the reactions better than complexed copper. It also indicates that the copper PyMACs are far less effective than the analogous nickel and iron systems. We did, however, obtain valuable insights on the chemistry governing this family of PyMACs by probing the CuLCOOH's solution and solid-phase protonation equilibria, which will be useful for isolating and studying the analogous iron complex, FeLCOOH.

keywords: bleomycin; peroxide activation catalysis; ABTS (2,2'-azino-bis(3-ethylbenzothiazoline-6-sulphonic acid); PyMAC (pyridine-aza macrocycle)

1. Introduction

Metallobleomycin is a glycopeptide that induces DNA strand scission upon oxygen binding to its metal center. Iron is typically employed, but copper and cobalt analogues are also of interest.¹⁻³ Researchers study bleomycin's properties, both as an anticancer agent and as an oxygen-activating system. With respect to the second application, various families of bleomycin model compounds have been synthesized for the purpose of probing their oxidation properties. One such family is the 2,12-dimethyl-3,7,11,17-tetraazabicyclo[11.3.1] heptadeca-1 (17),13,15-triene aminopyridine macrocycle, commonly known as CR, and its derivatives.⁴ First synthesized by Daryle Busch's research group in 1969, the nickel-containing macrocycle has been used as a template for reduction, functionalization and transmetallation.

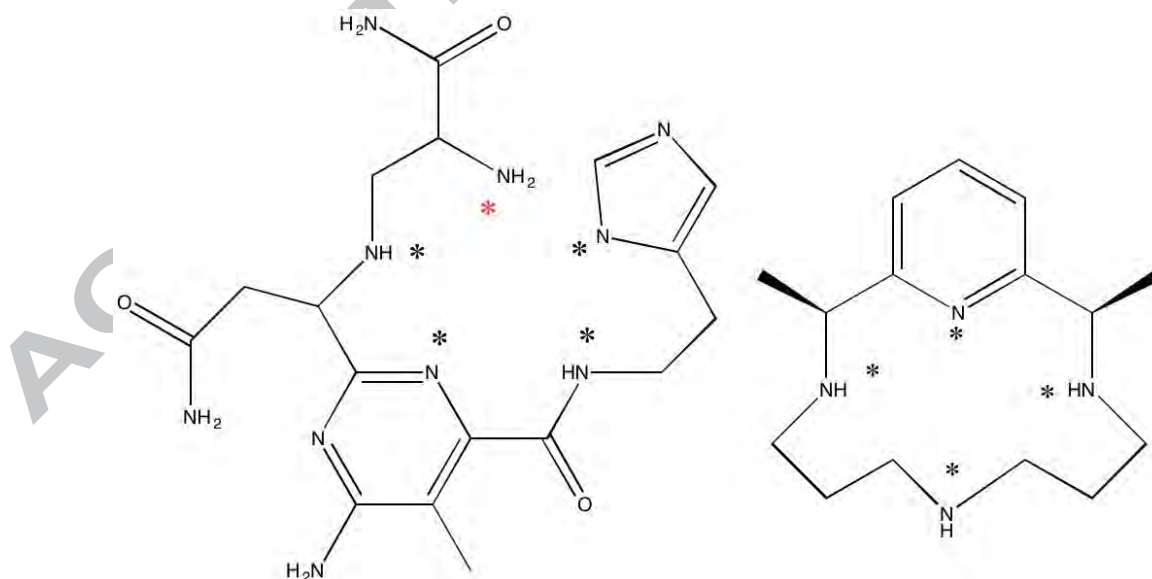


Figure 1. Comparison of the bleomycin (BLM) active site (left) to that of our CRH bleomycin mimic (right). Their respective coordination spheres are highlighted using asterisks, with BLM's axial amine highlighted in red.

Macrocycles with pendant arms attached are particularly interesting, as these functionalities often coordinate the metal center, boosting or inhibiting the complexes' activity.⁵⁻¹¹ Bleomycin's axial amine, shown in Figure 1, drives much of its reactivity; hence the inspiration for successive work on BLM models containing various pendant functionalities. We noticed with the nickel family of macrocycles that attaching carboxylic acid, amine and amide moieties to the square planar ligands boosted their oxidative reactivity towards the ABTS substrate, with the carboxylic acid- appended complexes being most effective.¹²

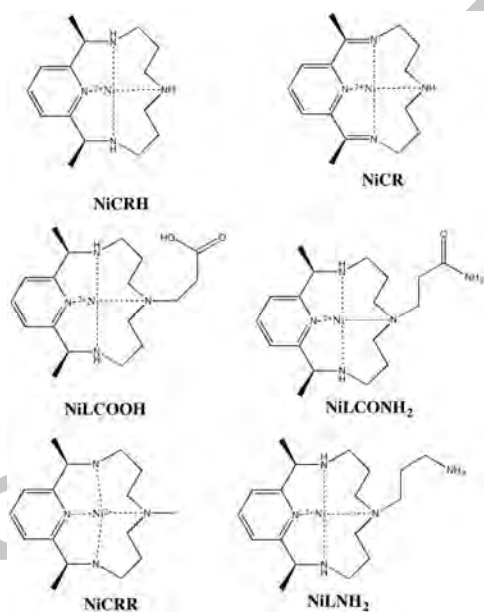


Figure 2. Selected nickel PyMACs appended with various functionalities.

Our previous work with carboxylic acid and amine-functionalized pyMACs revealed that the iron and nickel complexes underwent proton-deprotonation equilibria, shown in Figure 3.2, which strongly influenced

their olefin epoxidation capability. More specifically, protonating the catalysts' pendant arms drastically improved their oxidative ability.^{19,34}

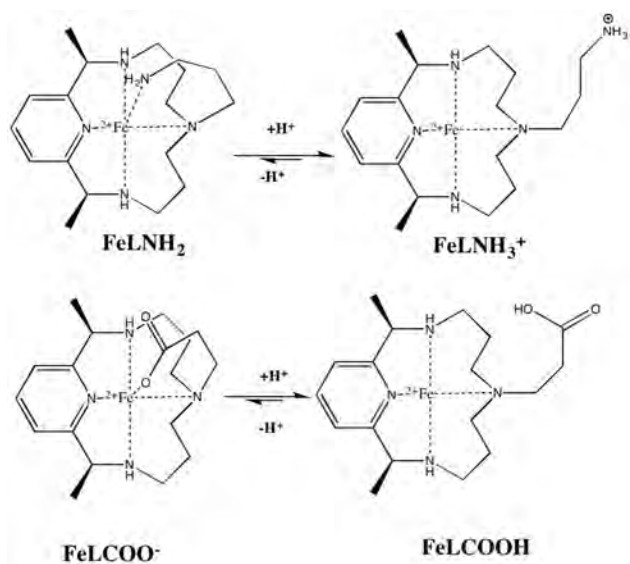


Figure 3. Comparison between the iron propylamine and carboxylic acid pymacs, showing their protonation/deprotonation equilibria. In both systems, the protonated species is catalytically active, while the deprotonated one is ineffective. (adapted from references 19 and 34).

Despite publishing an account of the FeLNH₂'s structural characterization and reactivity, our FeLCOOH work isn't quite complete.¹⁹ Repeated efforts to crystallize the fully protonated complex have been unsuccessful. Hence, our copper analog, CuLCOOH, serves as a proxy to shed some light on the protonation-deprotonation equilibria of the carboxylic acid functionalized complexes, given copper's superior stability to the other first-row transition metals.⁴⁴ We hoped that this would enable us to develop a useful method of isolating FeLCOOH. Our characterizations, which are the main discussion in this account, entail FTIR spectroscopy and X-Ray crystallography to determine the protonation state in solid form, as well as acid-base spectrophotometric titration to probe CuLCOOH's solution-phase behavior.

We also screened the complexes, and their corresponding perchlorate salt controls, for peroxidase, olefin epoxidation, and phenol oxidation activity.

2. Methods

2.1 General Considerations

Reagents were obtained from commercially available sources and used without further purification. The CRH and LCOOH ligand, and CuCRH complex were synthesized according to established literature procedures.¹²⁻

15

NMR spectra were obtained on the Bruker Avance III 500 spectrometer, using the Topspin 2.1 software. Electrospray ionization mass-spectra (ESI-MS) were taken via the Finnigan LTQ mass spectrometer using the LTQ Tune software. Gas chromatography analyses were performed on the Shimadzu QP-5050A GC-MS, using a DB-5 silica column. UV-Vis runs were done via the JASCO V-570 spectrophotometer's Spectra Manager program. Infrared spectra were obtained on the Nicolet Magna 760 FTIR's OMNIC software. X-Ray crystal structures were obtained using the Bruker D8 Quest X-Ray Diffractometer's APEX 2 software.

Caution! *Perchlorate salts of metal complexes with organic ligands are potentially explosive. Only small amounts of material should be prepared, and these should be handled with great caution.*

2.2 CuLCOOH Synthesis

89 mg (0.115 mmol) of copper (II) perchlorate hexahydrate was dissolved in 25 mL of DI water. 80 mg (0.115 mmol) of LCOOH ligand was

dissolved in 25 mL of ethanol, and the two solutions were mixed in a 100 mL 3-neck roundbottom flask at 65-70 °C for two to four hours. Complexation occurred instantly upon mixing, turning the solution navy-blue. Following the reaction, the mixture was rotavapped to dryness, dissolved in approximately 10 mL of hot water (~70-75 °C), filtered under vacuum to remove insoluble impurities, and then treated with ~1 mL of 70% perchloric acid.

The system was slowly cooled to room temperature, and the CuLCOOH crystals were filtered out and then washed with minimal cold ethanol and diethyl ether. They were then set to dry in a vacuum desiccator. The purified compound was characterized via ESI-MS (m/z 396 = [CuLCOOH-H]⁺). (Yield = 65.5%) CHN elemental analysis: Calculated: C = 34.16% H = 5.41% N = 8.85% Found: C = 33.98%, H = 4.74%, N = 8.02%) for C₁₈H₃₄Cl₂CuN₄O₁₂.

2.3 FTIR Spectroscopic Analysis

The FTIR spectrum of CuLCOOH was obtained in KBr pellets.

2.4 X-Ray Crystallography Studies

Saturated acetonitrile solutions of CuLCOOH were prepared and single crystals were isolated via slow-ether diffusion, before being structurally characterized.

All non-hydrogen atoms were refined anisotropically and all hydrogen atoms bound to carbon were included at geometrically calculated positions and refined using a riding model. The isotropic displacement parameters of all hydrogen atoms were fixed to 1.2 times the U_{eq} value of the atoms they

are linked to (1.5 times U_{eq} for methyl groups). Unless otherwise noted, all hydrogen atoms bound to electronegative elements (N, O) were found in the difference Fourier map and isotropic displacement parameters were fixed to either 1.2 (N–H) or 1.5 (O–H) times the U_{eq} value of the atoms they are linked to.

For $[\text{CuLCOOH}](\text{ClO}_4)_2 \cdot \text{H}_2\text{O}$, O–H (1,2-) and H–H (1,3-) distance restraints were applied to the lattice water molecule using the DFIX command. DFIX restraints on amine N–H distances were disagreeable and thus were not applied. The carboxylic acid hydrogen atom (H2O) was included in a calculated position using the HFIX 147 command. Similarity restraints (SADI) on 1,2- and 1,3-distances were applied to the two perchlorate ions in the asymmetric unit. No disorders were incorporated into the model.³⁴

2.6 Spectrophotometric Titration of CuLCOOH

A 2.8 mM aqueous solution of CuLCOOH was prepared. 2 mL of the solution were titrated with 0.25 equivalent increments of 0.089 M NaOH (7.87 L per increment), using a micropipette. The cuvette was shaken thoroughly to ensure proper mixing and changes in the UV-Vis absorption spectrum from run to run were observed, on the JASCO V-570. ($\lambda_{\text{max}} = 582$ nm, $\epsilon_{\lambda} = 119 \text{ M}^{-1}\text{cm}^{-1}$). This process was repeated with fresh CuLCOOH solution and 0.07 M perchloric acid, added in 10 μL increments with a micropipette.

2.7 ABTS Oxidation Catalysis Screening Experiments

All solutions were aqueous. 1.4 mM solutions of the ABTS substrate and the various complexes were prepared.

The oxidant was prepared from a 50% H₂O₂ solution, purchased from Sigma Aldrich containing a tin-based stabilizer, diluted to 88.2 mM.

Solutions of the ABTS substrate, the H₂O₂ oxidant, and the various complexes were prepared (0.0882M for H₂O₂ and 0.0014M for the substrate and catalysts respectively). Stoichiometric amounts of the substrate and catalyst (0.5 mL, each) were mixed with excess oxidant (0.5 mL) in a quartz spectrophotometric cuvet. The reaction was then studied in quintuplicate for 1000 seconds per run, via the JASCO V-570 UV-Vis spectrophotometer with the spectrophotometer, tuned to 420 nm, the absorption maximum of the ABTS radical cation.

2.8 Cyclooctene Epoxidation Experiments

The substrate: internal standard solution was prepared in a ratio of 2.5:1 of cyclooctene to chlorobenzene. 4.06 mL (0.04 mol, 4.50g) of the pure chlorobenzene internal standard and 13.03 mL (0.1 mol, 11.02 g) of the cyclooctene substrate were added to a volumetric flask and prepared as a 25 mL acetonitrile solution. A 3.2 mM solution of CuLCOOH catalyst was prepared in 25 mL of acetonitrile.

Fifteen gas chromatography vials were arranged in three rows of five and labeled Rows A, B and C. 1 mL of diethyl ether was added to each vial in Rows B and C. 40 µL (16 µmol) of the standardized cyclooctene solution were added to 1 mL of acetonitrile in each vial in Row A. 25 µL (0.08 µmol) of the

CuLCOOH catalyst solution were added to four of the Row A vials. Various equivalents of glacial acetic acid were added to each vial in Row A (0, 3, 6, 30 and 60 equivalents; 0, 2.75, 5.5, 27.5, and 55 μL , respectively) via micropipette.

5 μL of each Row A solution were transferred to the parallel Row B and C vials. 15 μL of H_2O_2 (300 equivalents) were added to the Row C vials, over five-minute periods, using a microsyringe.

The vials in Rows B and C were then analyzed to observe formation of cyclooctene oxide. The cyclooctene, chlorobenzene and cyclooctene oxide have retention times of approximately 6.125, 5.45 and 9.125 minutes, respectively.

3. Results and Discussion

3.1 CuLCOOH Characterization

3.1.1 Fourier Transform Infrared Spectroscopy

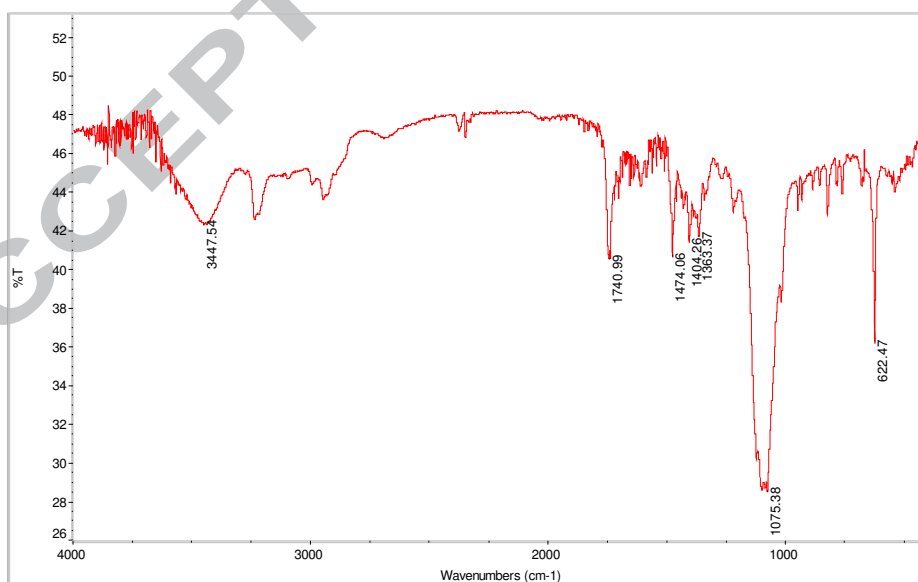


Figure 4. Fourier Transform Infrared spectrum of CuLCOOH. Carbonyl

(1740 cm^{-1}), alcohol ($\sim 2800\text{-}3000\text{ cm}^{-1}$) and perchlorate bands (~ 1075 and 622 cm^{-1}) are observed.

Figure 4 shows that CuLCOOH is fully protonated in its default state as indicated by the carboxylic acid carbonyl and alcohol bands at 1740 cm^{-1} and ($\sim 2800\text{-}3000\text{ cm}^{-1}$), respectively, as opposed to $\sim 1600\text{ cm}^{-1}$ for the carboxylate form.

3.1.2 X-Ray Structure Analysis

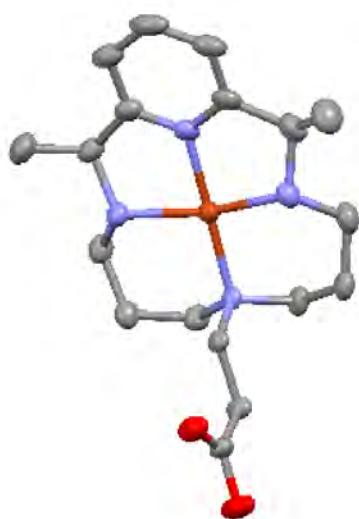


Figure 5. Thermal ellipsoid plot of CuLCOOH. Hydrogen atoms, perchlorates and water molecules are removed for clarity. The crystallography data indicate that CuLCOOH is fully protonated in the solid phase, corroborating our FTIR results.

3.1.3 Determining the CuLCOOH Protonation State

As shown in Figure 6, below, addition of 0.25- 1 equivalents of perchloric acid did not change the maximum absorbance or maximum wavelength (582 nm , $\epsilon_{\lambda} = 119\text{ M}^{-1}\text{cm}^{-1}$) of the CuLCOOH UV-Vis absorption spectrum. However, incremental addition of sodium hydroxide slightly diminished the absorbance, and shifted the λ_{max} from 582 nm to 586 nm ,

indicating that the starting complex is fully protonated in the solution phase, which aligns with the FTIR and X-Ray crystallography results. Additionally, the deprotonation-protonation equilibrium is reversible.

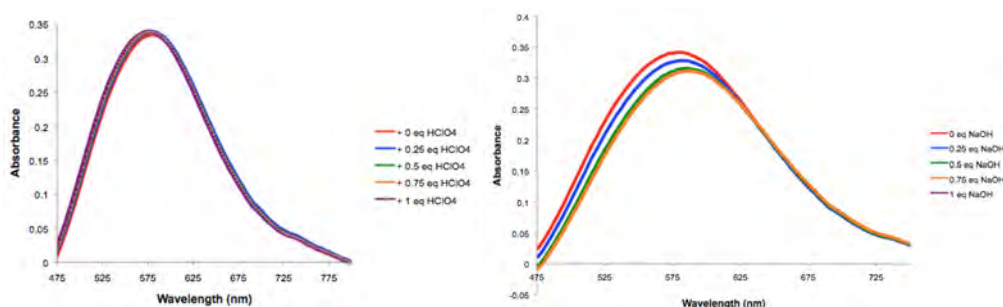


Figure 6. a) Acid and b) base spectrophotometric titration of 2.8 mM CuLCOOH, with 70 mM HClO₄, and 89 mM NaOH, respectively, in aqueous solution at room temperature. The maximum absorption shrinks slightly with each addition of base, but remains consistent with each increment of acid.

3.2 ABTS Oxidation Catalysis Screening

ABTS is a common substrate used in biochemistry research to assess the peroxidase properties of various enzymes and enzyme model systems. It readily undergoes a one-electron oxidation in the presence of hydrogen peroxide and a metal catalyst, forming a deep-blue radical cation that absorbs strongly at 420 nm, as shown in Figure 10.¹⁶⁻¹⁸ Hence, we initially screen our copper pyMACs for peroxidase activity before experimenting with more resistant substrates like phenols and olefins.

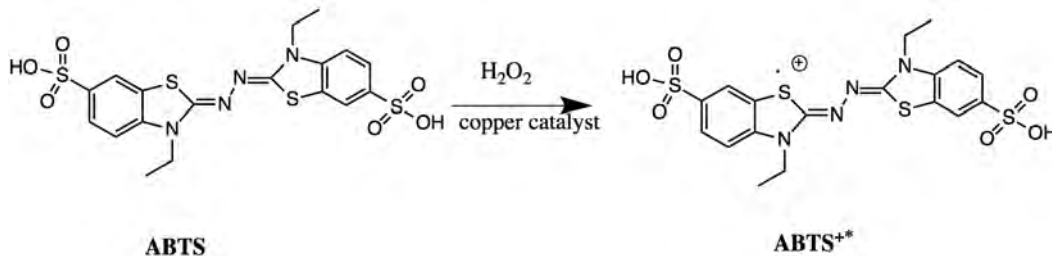


Figure 7. One-electron oxidation of ABTS by hydrogen peroxide in the presence of a copper catalyst, forming the radical cation, $\text{ABTS}^{+\cdot}$ ($\lambda_{\text{max}} = 420 \text{ nm}$, $\epsilon_{420} = 36000 \text{ M}^{-1}\text{cm}^{-1}$).

The carboxylic acid copper complex, CuLCOOH , demonstrated mild peroxidase activity. In contrast, the unfunctionalized copper complex, CuCRH , demonstrated no activity at all. Interestingly enough, the copper perchlorate control worked better than both experimental compounds. Robbins and Drago also noted a similar phenomenon, wherein copper tri- and tetradentate neutral amine and pyridine complexes were ineffective hydrogen peroxide activators. They hypothesized that the strongly bound multidentate ligands blocked the oxidant's coordination to the copper center.²¹ This might explain our copper complexes' catalytic inactivity.

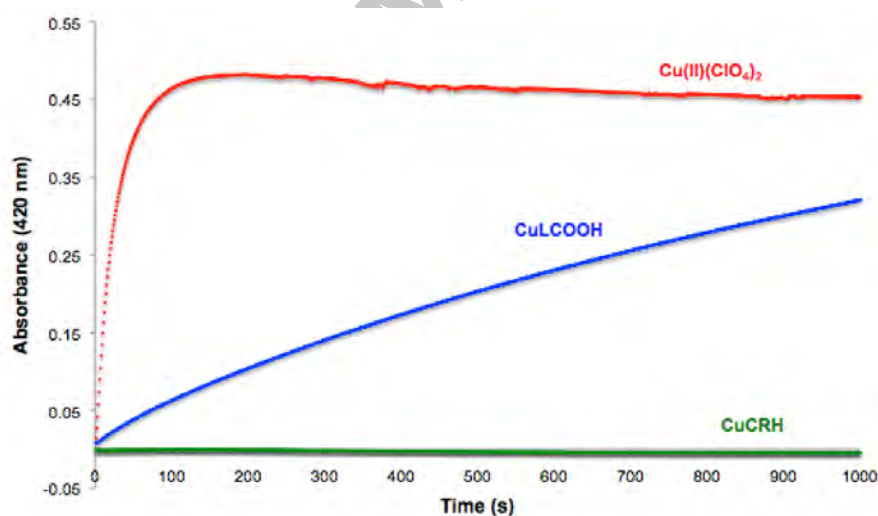


Figure 8. Comparison of copper complex peroxidase activity, no acid added. (1.4 mM copper catalyst, ABTS, 88.2 mM H_2O_2 , aqueous solution, room temperature, pH 5.7).

Adding acetic acid boosted the peroxidase activity of all three catalysts. This has been observed many times in oxidative catalysis work, though the exact mechanism is still up for debate.⁴⁰⁻⁴³ However, adding hydrochloric acid

diminished the activity of the complexes, but not the copper perchlorate control (see Figures S1 and S2).

Previous research shows that copper salts facilitate various oxidation reactions, ranging from cyclooctane and amino acid oxidation to porphyrin oxidative couplings to oxidative amine N-dealkylation.³⁵⁻³⁹ Hence, given that the copper salts outperformed the copper complexes in every reaction condition assessed, we speculated that free copper ions are responsible for their superior ABTS oxidation activity.²²⁻²⁶

3.3 Cyclooctene Epoxidation and Phenol Oxidation Catalysis

Neither the complexes nor the copper perchlorate salt exhibited any olefin epoxidation capacity. This stands in stark contrast to the analogous iron macrocycles. Even unfunctionalized iron complexes oxidized cyclooctene to some degree.²⁷

We also ran various phenol oxidation catalysis experiments using our copper complexes, none of which were successful. This was surprising, since copper (II) complexes are usually highly effective at catalyzing hydrogen atom transfer (HAT) reactions, with hydrogen peroxide as an oxidant.³¹⁻³³

Though our copper pyMACs were ineffective hydrogen peroxide activators, they revealed valuable insights into the chemistry behind this family of ligands, especially pertaining to their acid-base equilibria.

Apparently, the more stable first-row transition metal LCOOH complexes, copper and nickel, are easier to isolate in their fully protonated forms, especially if the starting reaction mixtures are acidified with the conjugate

acid of the MLCOOH 's counterion. We took this into account when synthesizing FeLCOOH , which will be detailed in a forthcoming paper.

The stark difference in peroxidase activity between CuLCOOH and NiLCOOH is also interesting, with the nickel complex being far more active (approximately $13.8 \mu\text{mol}$ vs $8.33 \mu\text{mol}$ of ABTS^{+*} were formed in the nickel and copper reactions, respectively) as shown in 2009.¹²

On the other hand, we observed the opposite phenomenon for the respective nickel and copper perchlorate salt controls. The nickel (II) perchlorate was catalytically inactive towards the ABTS substrate, whereas the copper (II) perchlorate behaved far better than the experimental complexes.¹² Though disappointing, this is supported by the scientific literature. Fenton chemistry of copper (II) salts has been documented in multiple different systems, which implicate various Cu(II) peroxo intermediates.²⁸⁻³⁰ The same is not true of nickel (II) salts. This difference in one-electron oxidation activity might be due to copper (II)'s extra d-electron granting it affinity for hydrogen peroxide activation.

Overall, it seems that our various PyMAC systems exhibit a tradeoff between stability and peroxide activation capacity, with $\text{Fe} > \text{Ni} > \text{Cu}$ in terms of reactivity, and the sturdier complexes being better suited to characterization analyses rather than catalytic studies. However, a broader scope of substrates and catalysts must be assessed in order to bolster or refute this hypothesis. Our ongoing synthetic and catalytic work with the analogous cobalt PyMACS may prove useful in this respect. Additionally, we

did not test catechol substrates during the copper studies, which might be fruitful experiments in the future.

Acknowledgments

The authors would like to thank Dr. Alexander Filatov of SUNY Albany for valuable discussions on X-Ray structure solution.

Funding

This work was supported by the U.S. Department of Energy (Grant DE-FG02-06ER15799 to E.R.A.) and National Science Foundation (Grant CHE 1412909). The NMR facility, the kinetic instrumentation, and the ESI-MS spectrometer at Tufts were supported by the NSF Grants CHE-MRI 0821508, CHE-CRIF0639138, and CHEM-MRI 0320783.

References

- [1] Hecht, S.M. *Acc. Chem Res.* 19 (1986) 383-391.
- [2] Stubbe, J. et al. *Acc. Chem. Res.* 29 (1996) 322-330.
- [3] Rao, E.A. et al. *J. Med. Chem.* 23 (1980) 1310-1318.
- [4] Karn, J.L., Busch, D.H., *Inorg. Chem.* 8 (1969) 1149-1153.
- [5] Archibald, S.J., *Annu. Rep. Prog. Chem., Sect. A* 104 (2008) 272-296.
- [6] Bukowski, M.R. et al. *Science.* 310 (2005) 1000-1002.
- [7] Kimura, E., *Pure Appl. Chem.* 58 (1986) 1461-1466.
- [8] Kimura, E. et al. *J. Am. Chem. Soc.* 109 (1987) 5528-5529.
- [9] Grapperhaus, C.A. et al. *Inorg. Chem.* 39 (2000) 5306-5317.
- [10] Nam, W., *Acc. Chem. Res.* 40 (2007) 522-531.
- [11] Sastri, C.V. et al. *Proc. Natl. Acad. Sci.* 104 (2007) 19181-19186
- [12] Organo, V.G. et al. *Inorg. Chem.* 48 (2009) 8456-8468.
- [13] Riley, D.P., *Inorg. Chem.* 14 (1975) 490-494.
- [14] Rusnak, L., Jordan, R.B., *Inorg. Chem.* 10 (1971) 2199-2204.
- [15] Lindoy, L.F. et al. *J. Coord. Chem.* 1 (1971) 7-16.
- [16] Walker, R.B., Everette, J.D., *J. Agric. Food Chem.* 57 (2009) 1156-1161.
- [17] Huang, D., Ou, B., Prior, R.L., *J. Agric. Food Chem.* 53 (2005) 1841-1856.
- [18] Ramirez, D.C., Gomez-Mejiba, S.E., Mason, R.P., *J. Biol. Chem.* 29 (2005) 27402-27411.
- [19] Taktak, S. et al. *Inorg. Chem.* 46 (2007) 2929-2942.
- [20] Herrera, A.M. et al. *Dalton. Trans.* 1 (2003) 846-856.
- [21] Robbins, M.H., Drago, R.S. *J. Cat.* 170 (1997) 295-303.

- [22] Hasegawa, E. et al. *Beilstein J. Org. Chem.* 9 (2013) 1397–1406.
- [23] Brennan, B.J. et al. *Chem. Commun.* 47 (2011) 10034–10036.
- [24] Ghosh, S.C. et al. *J. Org. Chem.* 77 (2012) 8007–8015.
- [25] Takehira, K. et al. *J. Chem. Soc. Chem. Commun.* 22 (1989) 1705-1706.
- [26] Takehira, K. et al. *Tetrahedron. Lett.* 30 (1989) 6691-6692.
- [27] Ye, W. et al. *Inorg. Chem.* 51 (2012) 5006–5021.
- [28] Kim, S. et al. *J. Am. Chem. Soc.* 137 (2015) 2867-2874.
- [29] Wellman, C.R., Ward, J.R., Kuhn, L.P., *J. Am. Chem. Soc.* 98 (1976) 1683-1684.
- [30] Cheng, L. et al. *Ind. Eng. Chem. Res.* 53 (2014) 3478–3485.
- [31] Karakhanov, E.A. et al. *Ind. Eng. Chem. Res.* 49 (2010) 4607–4613.
- [32] Lee, J.Y. et al. *J. Am. Chem. Soc.* 136 (2014) 9925–9937.
- [33] Shyamal, M. et al. *RSC Adv.* 4 (2014) 53520-53530.
- [34] Palluccio, W. Mechanistic Studies of Oxygen Activation and Atom Transfer Reactions with Mononuclear Vanadium(III), Iron(II), and Palladium(0) Complexes Ph.D. Thesis, Tufts University, 2014.
- [35] Hasegawa, E. et al. *Beilstein J. Org. Chem.* 9 (2013) 1397–1406.
- [36] Brennan, B.J. et al. *Chem. Commun.* 47 (2011) 10034–10036.
- [37] Ghosh, S.C. et al. *J. Org. Chem.* 77 (2012) 8007–8015.
- [38] Takehira, K. et al. *Tetrahedron. Lett.* 30 (1989) 6691-6692.
- [39] Kakinoki, S., Yamaoka, T. *Bioconjugate Chem.* 26 (2015) 639-644.
- [40] Mas-Ballester, R., Que, L., Jr. *J. Am. Chem. Soc.* 129 (2007) 15964.
- [41] Mas-Ballester, R. et al. *J. Mol. Catal. A.* 251 (2006) 49.
- [42] White, M. C.; Doyle, A. G.; Jacobsen, E. N. *J. Am. Chem. Soc.* 123 (2001) 7194.
- [43] Fujita, M.; Que, L., Jr. *Adv. Synth. Catal.* 346 (2004) 190.
- [44] Irving, H. M. N. H.; Williams, R. J. P. *J. Chem. Soc.* (1953) 3192–3210.

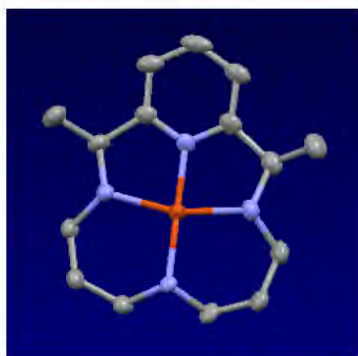
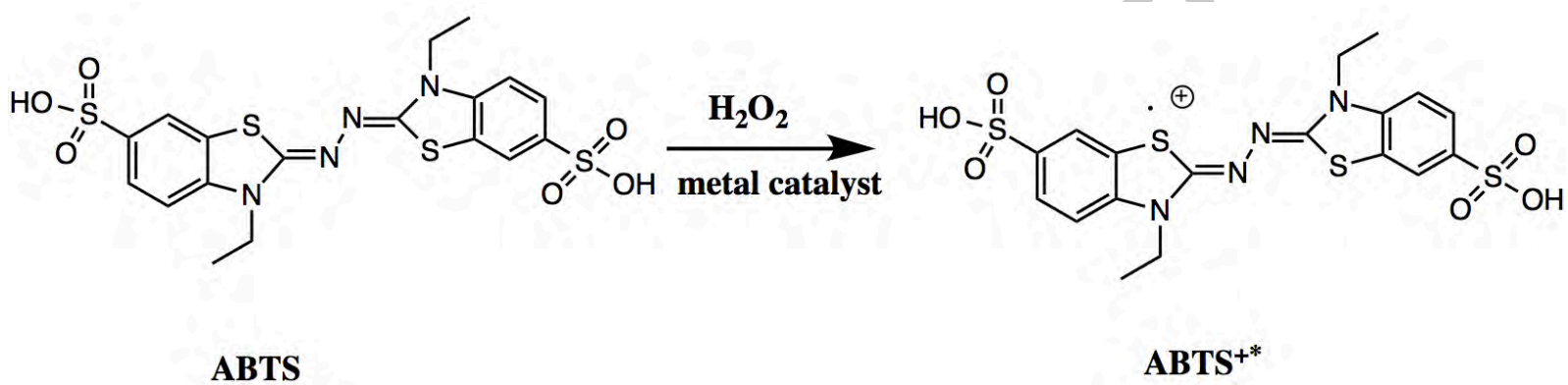
Competing Interests Statement

The authors have no competing interests to declare.

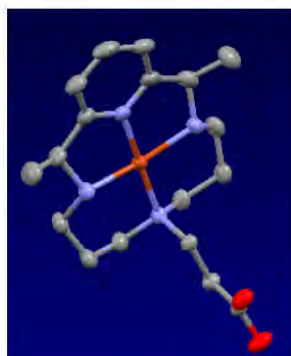
Author Information

Corresponding Author: Severin Garvey McKenzie

ACCEPTED MANUSCRIPT



^



^



AC

02132018 Highlights of "Synthesis, Characterization, and Oxidation Catalysis Studies of Monofunctionalized Copper Pyridine-Azamacrocycles"

- Functionalized pentadentate copper bleomycin (CuBLM) mimics were synthesized and characterized.
- Their peroxidase, and olefin and phenol oxidation properties were assessed.
- The copper (II) perchlorate control worked better than the experimental complexes.
- Characterization shed light on the protonation-deprotonation equilibria of this ligand family.